

# Characteristics of codried products of microcrystalline cellulose with saccharides and low-substituted hydroxypropylcellulose

Hsiu-O Ho, Chien-Ming Hsieh, Ming-Thau Sheu\*

Graduate Institute of Pharmaceutical Sciences, Taipei Medical University, 250 Wu-Hsing Street, Taipei 110, Taiwan, ROC

Received 21 June 2001; received in revised form 23 January 2002; accepted 26 March 2002

## Abstract

Codried products of microcrystalline cellulose (MCC) with saccharides (glucose, mannitol and sorbitol) and low-substituted hydroxypropylcellulose (L-HPC) of various grades (LH11, -20, -21, -22 and -31) were prepared. Their characteristics were evaluated and compared with the corresponding physical mixtures (PM) and dried product of MCC slurry (MCC-S). Improvement in flowability and Carr's index was demonstrated for codried products. Tablets prepared from most of the codried products showed a lower yield pressure and a shorter disintegration time, but a lower tensile strength. The  $E_0$  value of MCC-S was the highest among all MCC products tested. Further, all codried products demonstrated a lower  $E_0$  value than that of the corresponding physical mixtures. The extent of modification on the stiffness of MCC by L-HPC was larger than that by saccharides.  $K_{ic0}$  values for physical mixtures were larger than those of the corresponding codried products and MCC-S. On the other hand,  $K_{ic0}$  values for codried products of MCC with saccharides were in a comparable range of 0.63–1.10 MPa  $m^{1/2}$ , whereas that for codried products of MCC with L-HPC increased with increasing particle size (LH11 > LH21 > LH31).  $R_0$  was larger for physical mixtures than for the corresponding codried products. Most physical mixtures had a larger value of  $R_0$  than MCC-S except that for PMS, whereas values for most of codried products were smaller than that of MCC-S except for CD11 and CD21. The values of  $\sigma_{T0}$  for the codried products were lower than those for the physical mixtures, and both were lower than that for MCC-S. In terms of physical mixtures, the extent of decrease by mixing MCC with L-HPC was lower than that when mixing MCC with saccharides. However, the extent of decrease by codrying MCC with saccharides was greater than that with L-HPC. In conclusion, rounder, smoother particles with fewer free-moving fibers on the surface are the determining factor influencing the mechanical performance of the resulting codried products.

© 2002 Elsevier Science B.V. All rights reserved.

**Keywords:** Microcrystalline cellulose; Codried products; Particle morphology; Mechanical property; Low-substituted hydroxypropylcellulose; Saccharides

## 1. Introduction

Microcrystalline cellulose (MCC) is derived from purified wood  $\alpha$ -cellulose by severe acidic hydrolysis, yielding cellulose with a degree of polymerization (D.P.) of about 200–300. Excellent compactibility and low chemical reactivity have made MCC become one of the most useful excipients for direct compression tableting. The compactibility of MCC is mostly offered by plastic deformation and mechanical interlocking between particles [1]. However, the irregular shape, which contributes to interlocking bonding, results in poor flowability of MCC. In order to increase powder flowability and reduce weight variation of tablets, granulation is often recommended

when MCC is used in tablet formulations. However, a dramatic decrease in the compactibility of MCC has been reported when MCC is subjected to wet granulation [2]. Meanwhile, the compressibility of MCC is also negatively influenced by the slugging method as reported by Beten et al. [3].

According to Bavitz and Schwartz [4], the functionality of MCC can be modified by blending with starch, lactose and dicalcium phosphate, or by codrying with starch, calcium sulfate, etc. However, all these modifications offer direct compression tableting performance that falls short of that for MCC alone. A previous study reported that a codried product of MCC slurry with  $\beta$ -cyclodextrin ( $\beta$ -CD) had better compactibility, powder flowability and disintegration properties than did either existed commercially available MCC products codried with  $\beta$ -CD, dried MCC slurry alone or their physical mixtures with  $\beta$ -CD [5]. Advantages of using a codried process to improve the

\* Corresponding author. Tel./fax: +886-2-23771942.

E-mail address: mingsheu@tmu.edu.tw (M.-T. Sheu).

physical properties of MCC products containing MCC slurry and  $\beta$ -CD for pharmaceutical use were also demonstrated in this previous study. The possible mechanisms responsible for this improvement might be due to the hydrophilic wicking effect of  $\beta$ -CD and its ability by hydrogen bonding to intimate contact with MCC slurry during codrying process. Therefore, saccharides or L-HPC, both of which have basic molecular structures similar to that of MCC and with different ability by hydrogen bonding to interact with MCC, were selected for examination. Ultimately, the aim of this study was to evaluate the significant factors influencing physical characteristics of MCC by codrying MCC slurry with saccharides or L-HPC of various grades. Furthermore, mechanical performances of these codried products were compared with those of the corresponding physical mixtures.

## 2. Experimental methods

### 2.1. Materials

Wood pulp, Temalfa 94<sup>®</sup>, was obtained from Tembec (Canada). Low-substituted hydroxypropylcellulose (L-HPC) of various grades (LH11, -20, -21, -22 and -31) was supplied by Shin-Etsu Chemical (Japan). Saccharides, including glucose (dextrose anhydrous), sorbitol and mannitol, were pharmaceutical grade. The water solubility of three saccharides at 20 °C is in the following order: sorbitol (1 in 0.5) > glucose (1 in 1) > mannitol (1 in 5.5).

### 2.2. Preparation of the MCC slurry

First, 400 g of wood pulp was hydrolyzed in 3 l of 2.5 N HCl solution at 100 °C for 60 min. The hydrolyzed product was then washed with distilled water until the pH value of the washing solution was near neutral, and no white precipitation appeared with the addition of 0.1 N AgNO<sub>3</sub> solutions. The hydrolyzed product was next centrifuged to eliminate water. The final product, which retained about 50.0 ± 0.1% w/w of moisture, was designated as the MCC slurry. The DP value of this MCC slurry was about 230 and was measured according to NF 18.

### 2.3. Preparation of codried products and physical mixtures

The MCC slurry was blended with 10% w/w saccharides (including glucose (G), mannitol (M) and sorbitol (S)) or L-HPC (including LH11 (11), LH20 (20), LH21 (21), LH22 (22) and LH31 (31)), and these were mixed well by hand in a plastic bag. The mixtures were then transferred to a planetary mixer and granulated with a fixed amount of water (54.5% w/w) at a speed set at no. 2 until homogeneous. The wet mass was next sieved through a standard 30-mesh sieve, and the granules were dried at 60 ± 1 °C for 12 h. Dried granules were then milled and sieved to retain the

fraction between 60 and 150  $\mu$ m in size. The water content of granules was controlled to about 3–5%.

The MCC slurry was dried at 60 ± 1 °C for 12 h. Dried granules were then milled and sieved to retain the fraction between 60 and 150  $\mu$ m in size which was designated as MCC-S. Glucose, sorbitol, mannitol and L-HPC of various grades were pulverized and sieved to retain the same particle range as the dried granules of the MCC slurry (MCC-S). Physical mixtures were prepared simply by mixing the same ratio as that of codried products in a plastic bag with hand-shaking for at least 30 min. The water content of the mixtures was also controlled to about 3–5%.

### 2.4. Measurement of particle properties

#### 2.4.1. Flowability and Carr index

An A.B.D. Fine Particle Characteristics Measuring Instrument (Tsutsui Scientific Instruments, Tokyo, Japan) was used to determine the repose angle and the bulk and tapped densities of the particles. Carr's index was calculated as the ratio of the difference between tapped density and bulk density to tapped density.

#### 2.4.2. Particle morphology

Particle morphologies were examined under a scanning electron microscope (Hitachi model S-2400, Department of pathology, Taipei Medical University). Samples were loaded on aluminum studs and coated with gold for 3 min at 8 mA under a pressure of 0.1 Torr. The samples were scanned, and the micrographs were recorded.

### 2.5. Measurement of tablet properties

#### 2.5.1. Yield pressure

Flat-faced tablets of 12-mm diameter were compressed at 0.5, 0.75, 1.0, 1.25 and 1.5 metric tons by a Carver Hydraulic Laboratory Press with a raising rate of 0.5 cm/s and zero contact time. A total weight of 350 mg was prepared for each tablet. The diameter and thickness of tablets were recorded immediately after compression. Apparent particle density was determined in triplicate using a nitrogen–air pycnometer (Automated Gas Pycnometer, Model PYC-G100A-1). A Heckel plot (as shown in Fig. 1A and B) was then constructed, and the yield pressure was calculated as described previously [6].

#### 2.5.2. Tensile strength (TS)

Flat-faced tablets of 250 mg and 9-mm diameter were prepared at a compression force of 0.75 metric tons. The tablets were then stored for 1 week at a relative humidity of 40%. The load necessary to cause fracture was examined with a Pharma Test tablet hardness tester (Model PTB-311, Pharma Test, Germany). The tensile strength was calculated as follows:

$$\text{Tensile strength} = (2P)/(\pi Dt);$$

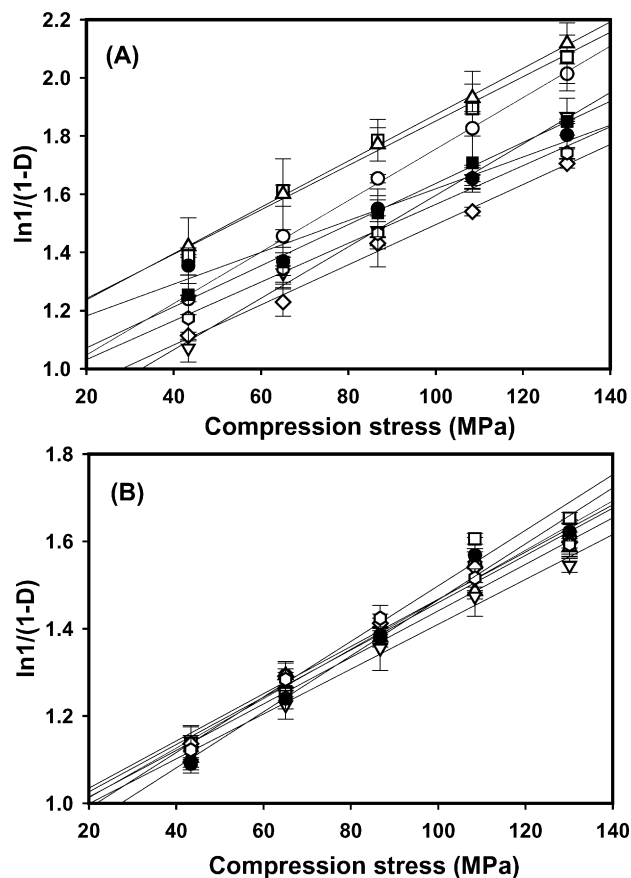


Fig. 1. Heckel plots for codried products (A) and physical mixtures (B) (○: CDG, PMG. □: CDM, PMM. △: CDS, PMS. ▽: CD11, PM20. ◇: CD21, PM21. ◊: CD31, PM22. ●: CD20, MCC-S. ■: CD22).

where  $P$  is the load necessary to cause fracture,  $D$  is tablet diameter and  $t$  is its thickness.

### 2.5.3. Rate constant of water uptake

Flat-faced tablets of 200 mg and 8-mm diameter were prepared at 0.5, 0.75, 1.0, 1.25 and 1.5 metric tons. The tablets were placed in a glass filter of a modified Enslin apparatus, similar to the apparatus designed by Ferrari et al. [7] and Nogami et al. [8]. The temperature of the water bath was maintained at 37 °C. The uptake volume of water at different time intervals was read from a graduated pipette and recorded. The rate constant of water uptake was calculated according to the following equation:

$$A = A_0 \times (1 - \exp^{-kt});$$

where  $A$  is the amount of water uptake (ml/g) at time  $t$ ,  $A_0$  represents the amount of water uptake at infinite time,  $k$  denotes the rate constant of water uptake and  $t$  is the elapsed time (s).

### 2.5.4. Disintegration

A total weight of 200 mg was prepared for each tablet with a compression force of 1.0 metric ton. Disintegration

was examined according to the United States Pharmacopoeia (USP XXIII) with six tablets for a period of 30 min at a temperature of  $37 \pm 1$  °C. The average of six tablets was reported.

### 2.6. Measurement of mechanical performance

All mechanical properties were determined using a three-point beam bending test on a dynamic mechanical analyzer (Perkin Elmer, Model DMA 7e, USA). Beams with or without crack were prepared by compacting the powders in a rectangular die, 25.4 mm in length and 5.13 mm in breadth in a Carver Hydraulic Laboratory Press with a raising rate of 0.5 cm/s and a contact time of 6 s. The thickness of the beams was controlled at 2 mm by the design of the depth of the upper punch. Since all beams were compressed to a constant thickness of 2 mm, porosity (0.13, 0.17, 0.21, 0.25 and 0.29) was varied by changing the weight of powder placed in the die cavity. All mechanical properties are influenced by the solid fraction of beams. By using Spriggs [9] equation, they were compared at zero porosity by extrapolating the plot of measured mechanical strength vs. porosity to 0. Young's modulus ( $E$ ) was obtained by stressing beams without crack to fracture at a frequency of 1 Hz. The maximum value of Young's modulus was recorded with a static force of 10 mN, a dynamic force of 8 mN, and a raising force of 200 mN/min. The critical stress intensity factor ( $K_{ic}$ ) and fracture toughness (FT) were determined by stressing beams with crack to fracture at the same experimental conditions of measuring  $E$  and calculated as described by Roberts et al. [10] and Mashadi and Newton [11], respectively, with the following equations:

$$K_{ic} = Y \frac{3FLc^{1/2}}{2wt^2}$$

$$Y = 1.93 - 3.07\left(\frac{c}{t}\right) + 14.53\left(\frac{c}{t}\right)^2 - 25.11\left(\frac{c}{t}\right)^3 + 25.8\left(\frac{c}{t}\right)^4$$

$$FT = \frac{F\delta/2}{wt - cw}$$

where  $F$  is the load caused the beam with crack to fracture,  $L$  is the distance between the supports,  $t$  is the thickness of the beam,  $c$  is crack length,  $Y$  is a function of the geometry of the specimen,  $w$  is the width of the beam and  $\delta$  is the displacement of probe of DMA.

## 3. Results and discussion

The particle properties are listed in Table 1 where demonstrates that the repose angle for all codried products falls between 32° and 34°, whereas that for the corresponding physical mixtures is larger than 40°. Comparably, Carr's index for codried products is in the range of 11–17%,

Table 1  
Physical characteristics of particles

Formulation	Repose angle (°)	Bulk density (g/ml)	Tapped density (g/ml)	Carr's index
<b>Codried</b>				
CDG	34.2 (2.5)	0.636 (0.002)	0.725 (0.003)	12.3 (0.1)
CDM	32.7 (0.3)	0.660 (0.003)	0.746 (0.002)	11.5 (0.4)
CDS	33.8 (0.3)	0.597 (0.003)	0.672 (0.001)	11.1 (0.4)
CD11	32.5 (0.5)	0.472 (0.001)	0.561 (0.002)	16.0 (0.2)
CD21	34.0 (1.0)	0.565 (0.010)	0.639 (0.005)	11.6 (2.1)
CD31	34.7 (0.6)	0.559 (0.010)	0.637 (0.004)	12.2 (1.2)
CD20	34.1 (0.2)	0.532 (0.013)	0.608 (0.002)	12.6 (2.3)
CD22	33.2 (0.3)	0.548 (0.006)	0.654 (0.003)	16.1 (1.0)
<b>Physical mixtures</b>				
PMG	41.0 (0.0)	0.288 (0.001)	0.387 (0.001)	25.5 (0.4)
PMM	40.3 (1.5)	0.287 (0.001)	0.389 (0.004)	26.2 (0.7)
PMS	39.0 (2.0)	0.281 (0.002)	0.382 (0.006)	26.5 (1.5)
PM20	42.3 (2.5)	0.263 (0.002)	0.373 (0.002)	29.5 (0.9)
PM21	45.0 (1.0)	0.267 (0.005)	0.362 (0.003)	26.3 (0.8)
PM22	44.3 (2.1)	0.260 (0.001)	0.357 (0.002)	27.2 (0.4)
MCC-S	43.7 (0.6)	0.271 (0.006)	0.364 (0.004)	25.7 (0.9)

whereas that for physical mixtures is between 25% and 30%. Both results indicate that codried products have better flowability than do physical mixtures. Scanning electric micrographs shown in Figs. 2 and 3 reveal that the difference in flowability was caused by the differences in particle shape. The particle shape of MCC after codrying is more regular with a smooth surface, whereas the corresponding physical mixtures are irregular with chipped edges.

Crystalline states of codried products were compared with those of physical mixtures by the examination of differential scanning calorimetry (DSC, Perkin Elmer, DSC-Pyris 1) in the temperature range between 30 and 200 °C with a heating rate of 10 °C/min. As shown in Fig. 4A, pure glucose melts at around 163 °C with a  $\Delta H$  of 186.8 J/g. A corresponding melting peak appears in a similar temperature range with a  $\Delta H$  of 17.69 J/g for the physical mixture of 10% glucose in MCC. The area under the curve of the melting peak was proportionally decreased and the shift of the melting peak was minimal. This indicates that glucose in the physical mixture retains the same crystalline state as pure glucose and a minimal interaction of crystalline form of glucose with MCC was expectable. Furthermore, no peak appears in this temperature range for the codried product of glucose with MCC. This means that glucose in the codried product is completely in an amorphous form as a result of the transformation of dissolved glucose to amorphous form during massing and drying step.

On the other hand, as shown in Fig. 4B and C, the melting peaks for mannitol and sorbitol at around 169 and 102 °C, respectively, appear in both thermograms of physical mixtures and codried products with the latter showing a smaller peak area. A partial transformation of crystalline mannitol and sorbitol into the amorphous form is demonstrated after codrying step. However, the shift of these two peaks with respect to the corresponding melting peak for crystalline form was minimal. It reveals that the intimate

interaction between sorbitol or mannitol and MCC in the codried products might expectedly be larger than that in the physical mixtures, but not so profound to cause an appreciable change in the bond strength. On the other hand, the formation of amorphous saccharides is mainly from the dissolved saccharides during drying step and the water solubility of glucose is not the highest among the three saccharides. Therefore, the difference in the extent of transformation of crystalline to amorphous form among three saccharides might be due to the difference in their characteristics of recrystallization. Glucose as a basic unit of MCC to induce a hindrance on recrystallization as a result of more intimate interaction between them might also be possible.

There shows no any obvious phase transitions in the DSC thermograms when the codried products of MCC with L-HPC of various grades were examined in the temperature range between 30 and 200 °C with a heating rate of 10 °C/min. The insolubility of L-HPC in water could be the reason to have such a low appreciable amount of L-HPC dissolved. Therefore, intimate interaction between MCC with L-HPC of various grades in the codried products could be more likely through some kinds of weak forces.

Physical characteristics of tablets from the physical mixture and the codried products, including yield pressure, radial tensile strength, disintegration time and rate constant of water uptake, are listed in Table 2. Most tablets prepared with the physical mixtures demonstrated higher values of radial tensile strength and higher yield pressures. However, these two parameters are comparable for the physical mixture and MCC-S. Tablets produced with codried products had a lower yield pressure with better compressibility. Moreover, the radial tensile strength of tablets produced from codried product of MCC with sorbitol was higher than those of MCC with the other two saccharides. Nevertheless, the radial tensile strength of tablets prepared with codried products of MCC with L-HPC was higher than those of MCC with the saccharides.

Since tablet strength of MCC is mainly attributed to the bonding surfaces of granules and the mechanical interlocking of fibers, particle shape would be a determining factor of tablet strength for the same range of particle sizes [5]. As indicated by SEM photographs, the particle shape of the codried products appears to be rounder and smoother than that of the corresponding physical mixture. Fiber-like structures are still observable for MCC-S and the physical mixtures. Rounder, smoother shapes of particles lead to fewer bonding surfaces for codried products, and fiber-like structures provide a greater extent of mechanical interlocking for MCC-S and the physical mixture. Therefore, this results in the tensile strength of tablets prepared with codried products being smaller than that of the physical mixtures.

In the disintegration test, the disintegration times for tablets prepared with codried products of MCC were shorter than those for the physical mixtures. In particular, tablets prepared from the codried products of MCC with L-HPC had a rapid disintegration rate. Tablets prepared with CDM



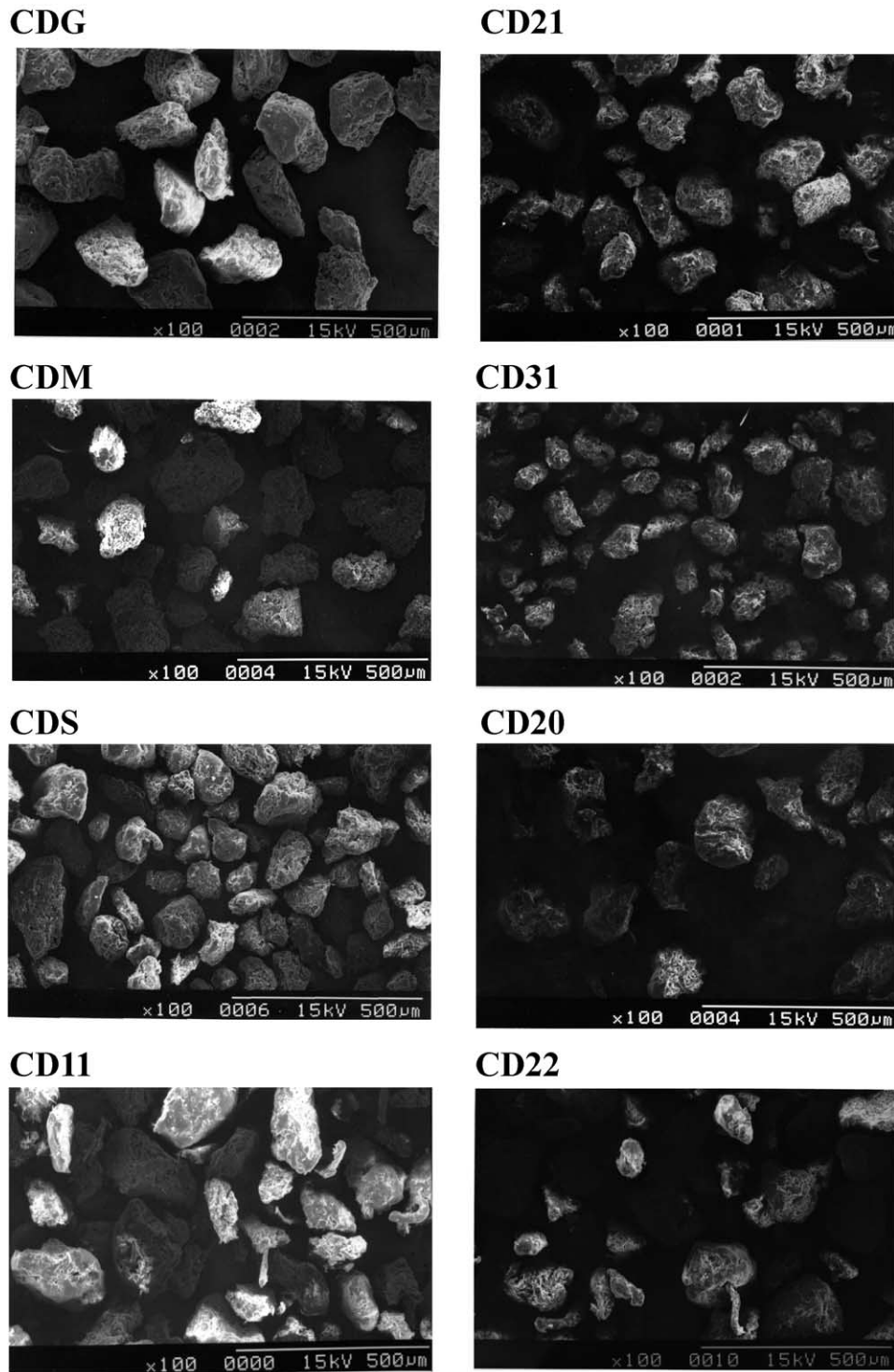


Fig. 2. SEM photographs of codried particles.

are the only codried products of MCC with saccharides to disintegrate within 30 min ( $3.9 \pm 0.9$  min). However, disintegration times for tablets produced from the physical mixtures were almost all over 30 min except those for PM20 ( $8.5 \pm 0.6$  min) and PM21 ( $13.5 \pm 2.1$  min). Lower tensile strength accompanied with higher porosity as an influential

factor to determine how fast water can penetrate into tablets should not be ignored.

In order to understand the mechanism of disintegration, the rate constant of water uptake ( $k_0$ , 1/s) and the amount of water uptake ( $A_0$ , ml/g) were compared at zero porosity, and the results are also given in Table 2. Tablets prepared with

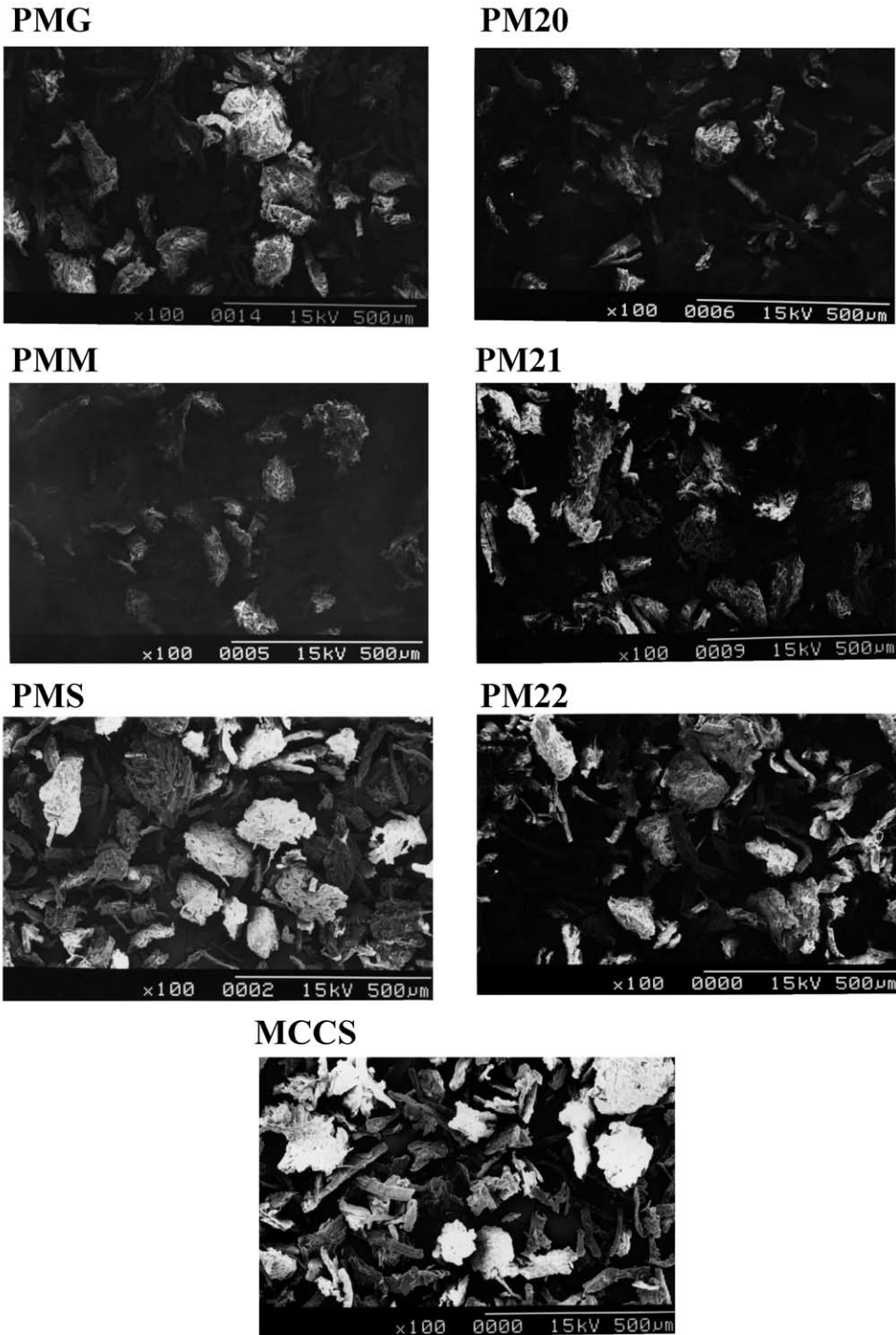


Fig. 3. SEM photographs of physical mixtures.

MCC-S show the fastest rate of water uptake. A lower rate constant of water uptake was observed for codried products of MCC with saccharides than for MCC with L-HPC. However, the amount of water uptake for tablets prepared with MCC-S was the smallest, whereas that for codried products was larger than those for the physical mixtures. Among tablets prepared from MCC with saccharides, that with CMM shows the highest rate constant of water uptake

for both codried product and the physical mixture. This also demonstrates that the rate constant of water uptake has a tendency to increase (LH11>LH21>LH31) with decreasing particle size (LH11 < LH21 < LH31) for codried products of MCC with L-HPC. As a result, tablets prepared from codried product of MCC with L-HPC LH31 show the largest rate constant of water uptake among all samples of either codried product or physical mixture.

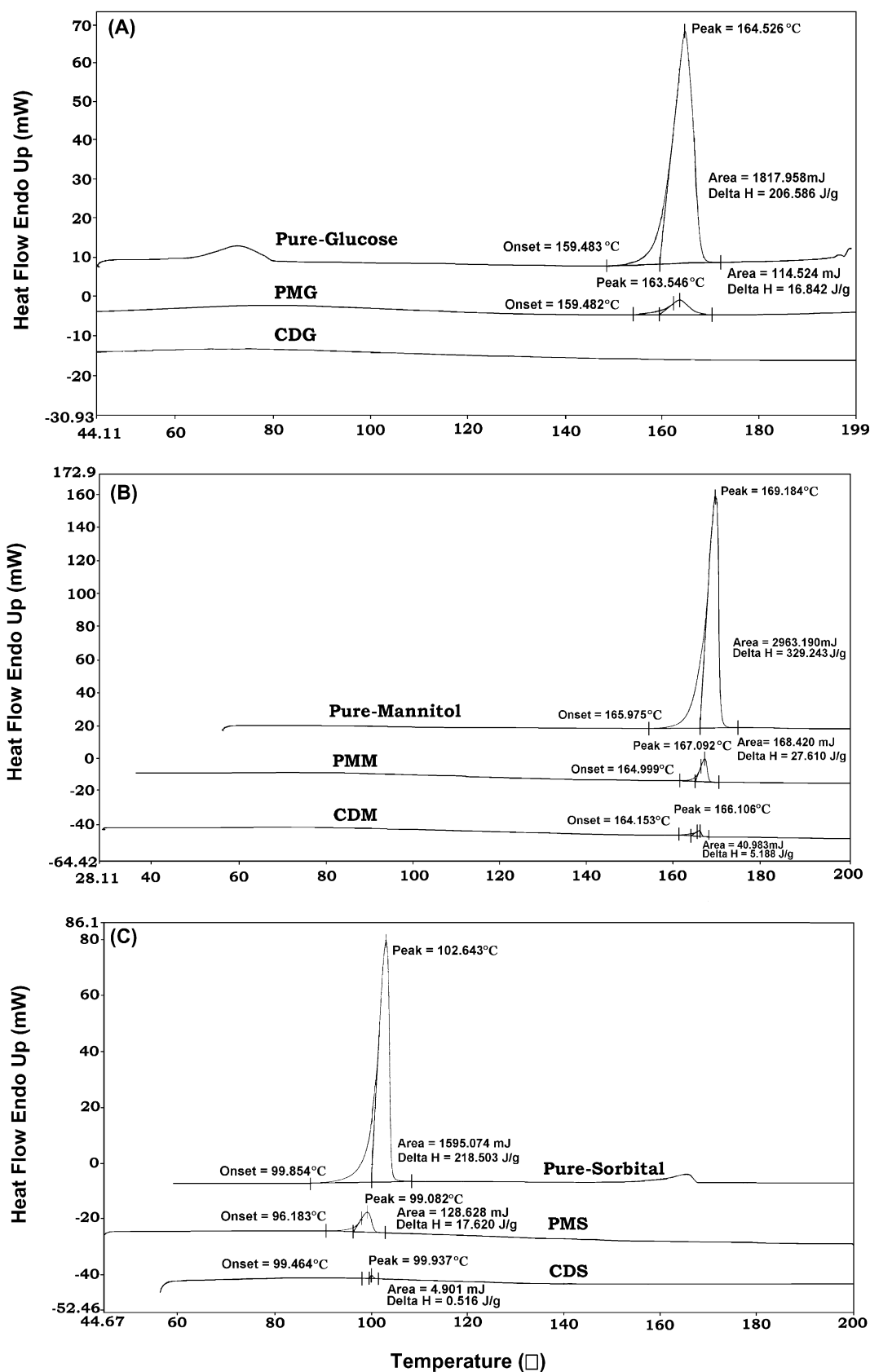


Fig. 4. DSC thermograms for glucose (A), mannitol (B) and sorbitol (C).

Table 2  
Physical characteristics of tablets

Formulation	Yield pressure (MPa)	TS (MN/cm <sup>2</sup> )	Disintegration time (min) <sup>a</sup>	ko (1/s)	Ao (ml/g)
Codried					
CDG	113.1 (2.70)	3.18 (0.11)	IV	$1.89 \times 10^{-6}$ ( $1.49 \times 10^{-6}$ )	0.939 (0.174)
CDM	131.2 (8.50)	2.31 (0.06)	I ( $3.89 \pm 0.78$ )	$5.49 \times 10^{-6}$ ( $1.08 \times 10^{-6}$ )	0.895 (0.103)
CDS	125.7 (1.60)	4.19 (0.23)	IV	$3.51 \times 10^{-6}$ ( $2.17 \times 10^{-6}$ )	0.888 (0.131)
CD11	113.2 (5.60)	3.60 (0.20)	II ( $5.29 \pm 0.67$ )	$1.58 \times 10^{-4}$ ( $8.28 \times 10^{-5}$ )	1.749 (0.260)
CD21	145.2 (7.10)	2.63 (0.09)	I ( $1.90 \pm 0.16$ )	$2.38 \times 10^{-4}$ ( $7.96 \times 10^{-5}$ )	1.856 (0.119)
CD31	150.0 (8.90)	2.65 (0.12)	II ( $7.67 \pm 1.41$ )	$3.55 \times 10^{-4}$ ( $2.05 \times 10^{-4}$ )	1.776 (0.118)
CD20	183.3 (21.9)	3.28 (0.32)	I ( $3.69 \pm 0.65$ )	$2.44 \times 10^{-5}$ ( $1.69 \times 10^{-5}$ )	1.701 (0.274)
CD22	141.5 (5.40)	3.10 (0.26)	I ( $1.50 \pm 0.12$ )	$2.17 \times 10^{-4}$ ( $1.04 \times 10^{-4}$ )	1.280 (0.116)
Physical mixtures					
PMG	176.5 (14.5)	7.48 (0.08)	V	$2.04 \times 10^{-6}$ ( $1.38 \times 10^{-6}$ )	0.812 (0.087)
PMM	157.1 (14.2)	7.01 (0.81)	V	$1.72 \times 10^{-5}$ ( $1.47 \times 10^{-5}$ )	0.719 (0.032)
PMS	187.6 (16.2)	7.94 (0.04)	V	$6.06 \times 10^{-7}$ ( $4.53 \times 10^{-7}$ )	1.074 (0.261)
PM20	194.6 (10.4)	7.84 (0.03)	II ( $8.45 \pm 0.60$ )	$1.20 \times 10^{-5}$ ( $6.21 \times 10^{-6}$ )	1.318 (0.097)
PM21	184.9 (15.4)	6.91 (0.36)	III ( $13.51 \pm 2.08$ )	$6.81 \times 10^{-5}$ ( $3.45 \times 10^{-5}$ )	1.270 (0.067)
PM22	184.7 (16.9)	7.98 (0.16)	V	$3.50 \times 10^{-6}$ ( $2.51 \times 10^{-6}$ )	1.033 (0.113)
MCC-S	155.9 (12.8)	7.62 (0.32)	V	$5.34 \times 10^{-4}$ ( $2.11 \times 10^{-4}$ )	0.699 (0.025)

<sup>a</sup> Criteria I: completely disappears within 30 min. Criteria II: disintegrates to more than five pieces at 30 min. Criteria III: disintegrates to less than or equal to four pieces at 30 min. Criteria IV: disintegrates to two pieces within 30 min. Criteria V: one or two small pieces separate from tablet within 30 min. Criteria VI: intact tablet after 30 min. Figures in parentheses indicate the time (mean  $\pm$  S.D.) required to disintegrate completely.

As disclosed above, the water solubility of the three saccharides at 20 °C is in the following order: sorbitol (1 in 0.5) > glucose (1 in 1) > mannitol (1 in 5.5). For tablets prepared with physical mixtures, the rate constant of water uptake decreases with the increasing water solubility of the saccharides. For tablets prepared with codried products, the rate constant of water uptake follows this same order except for glucose. This change is probably because amorphous glucose in the codried product is more soluble than crystalline glucose in the physical mixture. This correlates well with the disintegration of tablets at this same level of strength as shown in this study. We conclude that the disintegration of tablets prepared with MCC and saccharides is mainly controlled by the rate constant of water uptake. It has to be larger than a certain level to cause disintegration.

Although tablets prepared with MCC-S show the fastest rate constant of water uptake, their disintegration times appear to be more than 30 min. This indicates that the faster rate of water uptake for MCC-S is not dominantly responsible for making the tablet disintegrate. On the other hand, the tablet strength of MCC-S is at such a high level that it leads to further deterioration of disintegration. With no aid of extra force, such as swelling force, acting synergetically with capillary force inducing by a faster rate of water uptake, disintegration of tablets prepared with MCC-S is retarded expectedly. On the contrary, the disintegration time for tablets containing L-HPC regardless of being either codried product or physical mixture was shorter even though their rate constants of water uptake are smaller than that for MCC-S. It has been reported that the swelling volume for L-HPC is ten times larger than that for MCC [12]. Probably, swelling volume is a determining factor in this situation causing tablets to disintegrate at this level of tablet strength. We conclude that the swelling force caused

by L-HPC as previously reported is the main factor causing tablets prepared with L-HPC to disintegrate at a faster rate.

To understand the effects of saccharides and L-HPC on the characteristics of MCC at structural level, mechanical properties, including young's modulus ( $E$ ), critical stress intensity factor ( $K_{Ic}$ ), fracture toughness ( $R$ ), and tensile strength ( $\sigma_T$ ), of these codried products were measured and extrapolated to zero porosity using an exponential relationship. Comparisons were made with the corresponding physical mixtures and the results are listed in Table 3. Young's modulus at zero porosity ( $E_0$ ) as calculated in Fig. 5 stands for the stiffness of materials, with larger  $E_0$  values resulting in increasing stiffness. The critical stress intensity factor at zero porosity ( $K_{Ic0}$ ) as calculated in Fig. 6 indicates the brittleness of materials, with a higher  $K_{Ic0}$  resulting in lower brittleness and higher resistance to fracture. Fracture toughness at zero porosity ( $R_0$ ) as calculated in Fig. 7 illustrates the toughness of materials, with a larger  $R_0$  resulting in higher toughness.

As shown in Table 3, the  $E_0$  value of MCC-S was the highest among all MCC products including codried product and physical mixtures. Further, all codried products demonstrate a lower  $E_0$  value than their corresponding physical mixtures, indicating that codrying with various excipients decreases the stiffness of MCC. The extent of modification of the stiffness of MCC by L-HPC was larger than that by saccharides. The stiffness of codried products was comparable but at a lower level with no matter which grades of L-HPC was used. However, the stiffness of codried products with saccharides was higher and differed in the following order, glucose < mannitol < sorbitol. For these codried products with saccharides, there is an indication that increasing the extent of the amorphous form of saccharides in the codried mixture leads to lower stiffness. The influence of



Table 3  
Mechanical characteristics of tablets

Formulation	$E_0$ (GPa)	$K_{ic0}$ (MPa m <sup>1/2</sup> )	$R_0$ (N m <sup>-1</sup> )	$\sigma_{T0}$ (MPa)
Codried				
CDG	8.076 (1.908) <sup>a</sup>	0.633 (0.217) <sup>a</sup>	144.93 (40.03) <sup>a</sup>	23.91 (6.56) <sup>a</sup>
CDM	18.183 (2.109)	0.776 (0.776)	135.89 (40.18)	47.81 (8.81)
CDS	31.602 (7.558)	1.102 (0.381)	385.83 (147.89)	65.76 (10.53)
CD11	8.556 (1.067)	5.118 (1.488)	1034.08 (193.34)	31.43 (3.75)
CD21	6.684 (0.551)	2.296 (0.735)	818.25 (202.06)	22.62 (2.69)
CD31	7.160 (0.644)	0.770 (0.059)	99.30 (20.81)	34.41 (4.19)
CD20	5.240 (0.565)	1.097 (0.241)	63.18 (11.31)	31.09 (4.56)
CD22	6.155 (0.465)	0.756 (0.240)	131.90 (27.08)	25.29 (5.08)
Physical mixture				
PMG	30.263 (4.279)	3.116 (0.559)	1276.66 (468.64)	62.95 (10.88)
PMM	23.942 (6.987)	4.473 (2.592)	1292.07 (749.77)	92.29 (11.95)
PMS	27.241 (11.633)	1.655 (0.368)	586.47 (130.78)	108.65 (46.39)
PM20	20.335 (7.055)	3.754 (1.789)	1804.54 (1125.80)	143.39 (26.16)
PM21	29.324 (8.888)	2.855 (0.879)	971.69 (406.72)	130.73 (48.98)
PM22	23.212 (3.656)	5.483 (1.034)	2080.84 (739.04)	116.62 (36.54)
MCC-S	31.259 (7.576)	1.720 (0.147)	875.83 (454.23)	147.04 (65.16)

<sup>a</sup> Mean (S.E.).

porosity (probably extra granules) on the stiffness seems to be significant as shown in Fig. 1 in which as the porosity of all products increased there was a decrease in the stiffness. It is most likely that the change in the porosity is the result of the fraction of extra granules. In turn, the stiffness extrapo-

lated to zero porosity could be further dependent on the intragranular porosity. In terms of this, a material with more of the amorphous form would be easier to fit in the spacing of the MCC fibers. Therefore, this explains why the stiffness of codried products of MCC with saccharides follows this

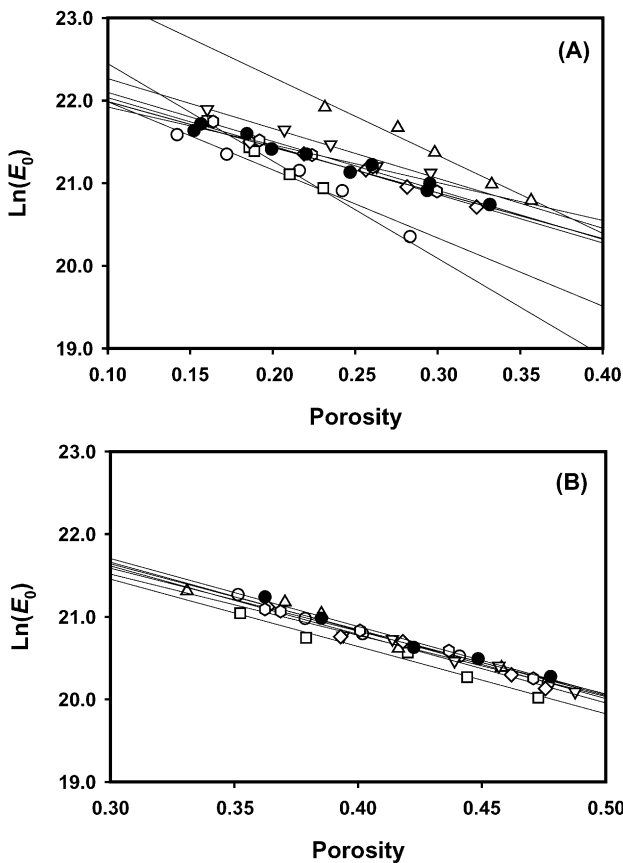


Fig. 5. Young's modulus ( $E$ ) versus porosity for codried products (A) and physical mixtures (B) (refer to Fig. 1 for keys).

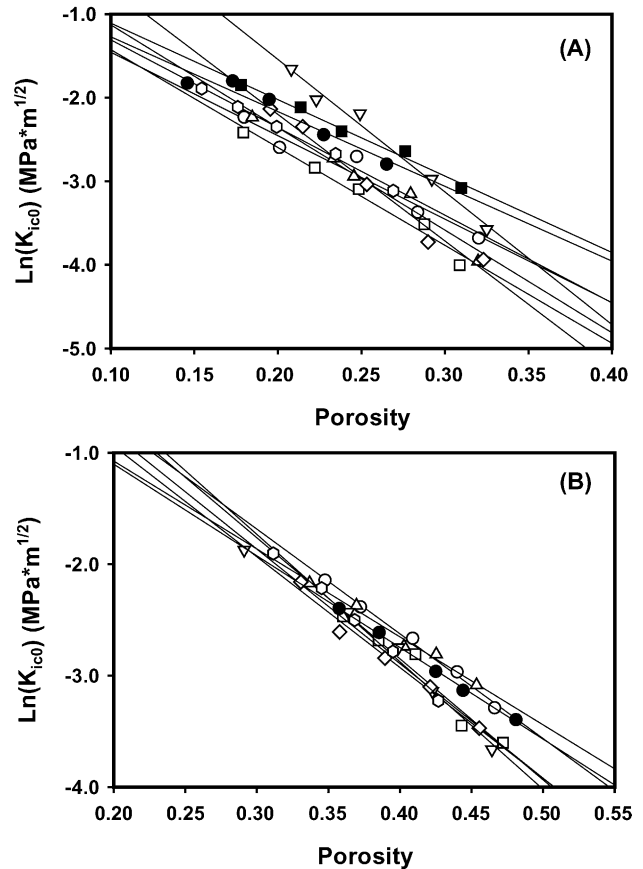


Fig. 6. Critical stress intensity factor ( $K_{ic}$ ) versus porosity for codried products (A) and physical mixtures (B) (refer to Fig. 1 for keys).

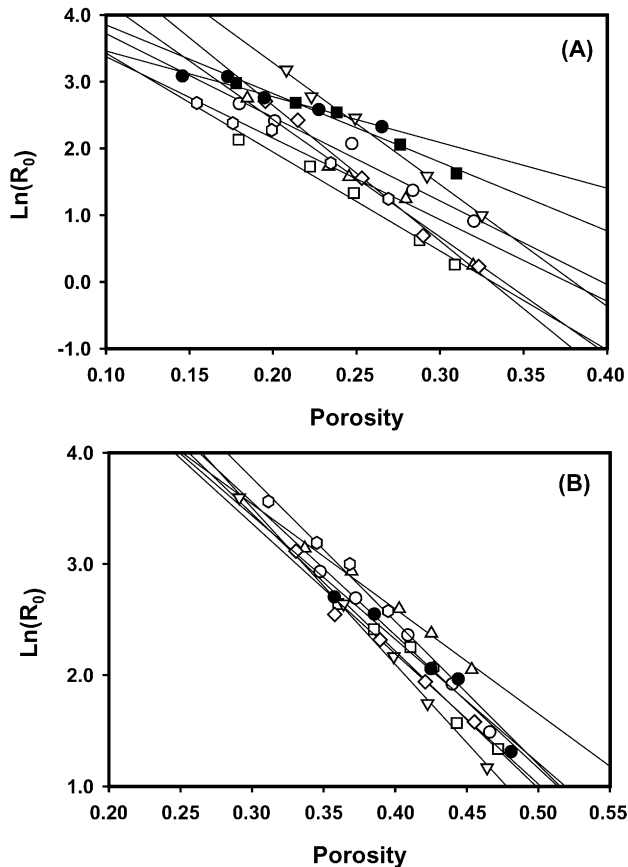


Fig. 7. Fracture toughness ( $R$ ) versus porosity for codried products (A) and physical mixtures (B) (refer to Fig. 1 for keys).

order. Similarly, fiber entanglement between MCC and L-HPC should not be close enough to create a greater extent of porosity inside the granules after codrying. This is why the stiffness of most codried products of MCC with L-HPC is lower than that with saccharides.

Results shown in Table 3 demonstrate that  $K_{ic0}$  values for physical mixtures were larger than the corresponding codried products and MCC-S. On the other hand,  $K_{ic0}$  values for codried products of MCC with saccharides were in a comparable range of  $0.63\text{--}1.10\text{ MPa m}^{1/2}$ , whereas that for codried products of MCC with L-HPC increased with increasing particle size (LH11>LH21>LH31). Since  $K_{ic0}$  value is an indicator of a material to resist crack propagation, a lower  $K_{ic0}$  value indicate that the codried process causes tablets prepared with these kinds of granules to become much more brittle. The effect is obviously greater for those tablets prepared with particles produced by codrying MCC with saccharides than that with L-HPC. Perhaps, codried particles of MCC with L-HPC still present more fiber-like structures on the surface (as shown by SEM) for bonding among particles leading to lower brittleness. Further shown by SEM, the extent of free-moving fibers on the surface of particles for bonding seems to increase with increasing particle size of L-HPC resulting in the  $K_{ic0}$  value increasing correspondingly. Further indicated by a larger

$K_{ic0}$  value, simply physically mixing MCC-S with saccharides or L-HPC produces a less-brittle material. This could be a result of the binding effect of saccharides or the interlocking effect of L-HPC in the physically mixed state.

Results in Table 3 further illustrate that  $R_0$  is larger for physical mixtures than for the corresponding codried products. Most of the physical mixtures had a larger value of  $R_0$  than MCC-S except that for PMS, whereas values for most of the codried products were smaller than that for MCC-S except CD11 and CD21. Also, the reduction of the  $R_0$  values for codried products of MCC with L-HPC became greater with increasing particle size (LH11>LH21>LH31). This obviously indicates that the codrying process leads to tablets with different extents of decreasing toughness. However, the physical mixing of MCC-S with either saccharides or L-HPC produces tablets with increasing toughness. The main differences between codried products and physical mixtures are the shape of particles and the crystalline status of the saccharides and L-HPC. Round, smooth particles would reduce the contact points between particles resulting in the ability of cracks to propagate along these weak points thus decreasing toughness. Therefore, the amorphous form of glucose or smaller-sized L-HPC particles (LH31) would be expected to easily reside in the spacing between the fibers of MCC resulting in either rounder and smoother-shaped

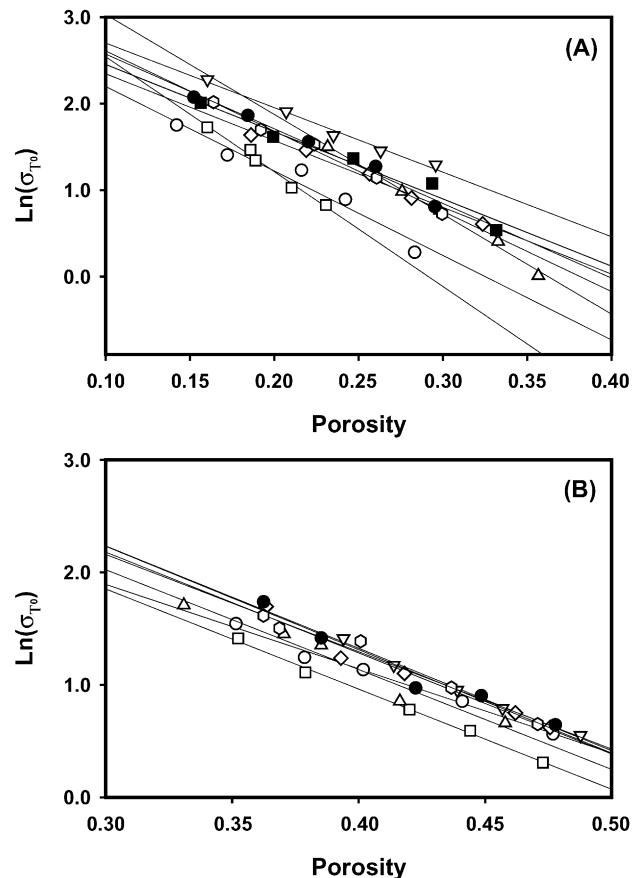


Fig. 8. Tensile strength ( $\sigma_T$ ) versus porosity for codried products (A) and physical mixtures (B) (refer to Fig. 1 for keys).

particles or fewer free-moving fibers on the surface of particles for interlocking.

Tensile strengths at zero porosity ( $\sigma_{T0}$ ) measured by the three-point bend test are also listed in Table 3 and were calculated as shown in Fig. 8. The values of  $\sigma_{T0}$  for codried products are lower than those for the physical mixtures, and both groups are lower than that for MCC-S. In terms of physical mixtures, the extent of decrease by mixing MCC with L-HPC is lower than that with saccharides. However, the extent of decrease by codrying MCC with saccharides is greater than that with L-HPC. It has been reported that the main factors attributed to the tensile strength of MCC tablets are the bonding surface area and the interlocking of fibers. The former is related to the shape, size and closeness of particles, whereas the latter is dependent on the extent of fiber-like structures retained by the materials. As shown by SEM photographs, round, smooth particles were produced after codrying as expected resulting in less bonding surface area and fewer fiber-structures for building-up tablet strength. Furthermore, amorphous form of glucose would cover the surface of MCC particles more efficiently leading to a greater reduction in tablet strength than with either sorbitol or mannitol.

#### 4. Conclusions

In conclusion, rounder, smoother particles with fewer free-moving fibers on the surface are the determining factor influencing the performance of the resulting codried products. Tablets produced from codried products of MCC with saccharides or L-HPC of various grades possess a lower, but acceptable, tensile strength and a lower yield pressure compared to those tablets produced from the physical

mixtures and original MCC material. Nevertheless, the efficiencies of both flowability and disintegration of codried products were improved. Although the codried product of MCC with sorbitol produced tablets with better flowability, higher hardness, and tensile strength, the disintegration time was too long and needs to be improved. Overall, codrying with L-HPC results in better performance of materials than that with saccharides, especially with grade LH11.

#### Acknowledgements

We would like to express our sincere thanks for the financial support of the National Science Council of the Republic of China (NSC 89-2320-B038-065).

#### References

- [1] C. Nyström, G. Alderborn, M. Duberg, P.G. Karehill, *Drug Dev. Ind. Pharm.* 19 (1993) 2143.
- [2] J.N. Staniforth, A.R. Baichwal, J.P. Hart, P.W.S. Heng, *Int. J. Pharm.* 41 (1988) 231.
- [3] D.B. Beten, N. Yuksel, T. Baykara, *Drug Dev. Ind. Pharm.* 20 (1994) 2323.
- [4] J.F. Bavitz, J.B. Schwartz, *Drug Cosmet. Ind.* 114 (1974) 44.
- [5] T. Tsai, J.S. Wu, H.O. Ho, M.T. Sheu, *J. Pharm. Sci.* 87 (1998) 117.
- [6] T. Pesonen, P. Paronen, *Drug Dev. Ind. Pharm.* 16 (1990) 591.
- [7] F. Ferrari, M. Bertoni, C. Caramella, M.J. Waring, *Int. J. Pharm.* 112 (1994) 29.
- [8] H. Nogami, T. Nagai, E. Fukuoka, T. Sonobe, *Chem. Pharm. Bull.* 17 (1969) 1450.
- [9] R.M. Spriggs, *J. Am. Ceram. Soc.* 44 (1961) 628.
- [10] R.J. Roberts, R.C. Rowe, P. York, *Int. J. Pharm.* 125 (1995) 157.
- [11] A.B. Mashadi, J.M. Newton, *J. Pharm. Pharmacol.* 39 (1987) 961.
- [12] Y. Bi, H. Sunada, Y. Yonezawa, K. Danjo, A. Otsuka, K. Iida, *Chem. Pharm. Bull.* 44 (1996) 2121.